

# Journal of Mechanics of Materials and Structures

A NONLINEAR STRESS-STRETCH RELATIONSHIP  
FOR A SINGLE COLLAGEN FIBRE IN TENSION

Francesco Genna

Volume 9, No. 5

September 2014





## A NONLINEAR STRESS-STRETCH RELATIONSHIP FOR A SINGLE COLLAGEN FIBRE IN TENSION

FRANCESCO GENNA

A new stress-strain equation for a single, stretched collagen fibre (bundle) is developed, based on the statistical description of the fibre microstructure, down to the tropocollagen molecule level. The derivation follows previous work of Annovazzi and Genna (2010), but the modifications reported here both simplify and improve the final result. The model is governed by physically meaningful parameters. Comparisons between the model predictions and some available experimental results suggest that the proposed model could be of value in bioengineering applications.

### 1. Introduction

In [Annovazzi and Genna 2010] (hereafter referred to as [AG]), a constitutive model for a single collagen fibre was derived on the basis of assumptions concerning both the fibre microstructure and the mechanical behaviour of the tropocollagen molecule. The present paper aims at simplification, improvement, and better internal consistency with respect to what done in [AG].

The main motivation for this work is the relative scarcity of constitutive models for the stress-stretch behaviour of a single collagen fibre in tension. The most commonly adopted assumptions for the collagen fibre constitutive law are in fact still not fully adequate. They might be either unrealistic, such as linear elasticity, or purely phenomenological, such as linear or nonlinear viscoelasticity, or hyperelasticity, based on the definition of potential functions that depend on parameters having no physical meaning. One reason for this could be the fact that the interest is often focussed on tissue analysis, so complicated in itself that it leaves little space for an accurate description of the underlying constituents, i.e., the single fibres. Examples of this type of difficulty can be found in [Grytz and Meschke 2009; Cacho et al. 2007; Wang et al. 1997; Limbert 2011].

To the best of our knowledge, only one attempt — that of [AG] — has been made at deriving a microstructurally based stress-stretch law for a single collagen fibre. This could cover the whole range of possible tensile loading, and described the microstructure of the fibre itself, which includes several levels of subcomponents, down to the molecular level [Kastelic et al. 1978]. The fibre stress-strain relationship presented in [AG] was based on the statistical description of the crimp properties of all the internal levels — four, according to the available information — of the fibre itself. The results obtained in [AG], however, could be improved in several respects:

- in the absence of data concerning the tropocollagen molecule, the equation for the elastic behaviour at the molecular level was taken, in [AG], from a model developed for a DNA molecule, an extension of the so-called WLC model of [Bustamante et al. 2000];

---

Work done within a research project financed by the Italian Ministry of Education and Research (MIUR)..

*Keywords:* collagen fibre, constitutive modelling, microstructure, statistical analysis.

- the failure of the tropocollagen molecule was described in [AG] on the basis of uncertain force data concerning the DNA molecule;
- the assumptions regarding the statistics of the waviness at the molecular level were inconsistent, in [AG], which resulted in needless analytical complications;
- crosslinking was ignored;
- all the subfibrils, at all the sublevels, were assumed to be continuous and stress-carrying, ignoring the existence of both interrupted subfibrils and of extra fibrous matter/voids;
- all the probability density functions for all the random variables, in [AG], were taken as Gaussian; this created some inconsistency in the definition of the governing parameters.

Here, a modification of the model of [AG] is presented. It overcomes the quoted problems and, at the same time, it is much simpler, and is better suited to be adopted even in large-scale applications, as shown in an accompanying paper [Genna and Paganelli 2014]. The main features of the constitutive model described here are of two types: those that follow what was already presented in [AG], and those which modify and improve the previous approach. In summary:

*Retained features:*

- a collagen fibre, or bundle, is seen as having an internal hierarchy of 4 sublevels of wavy or crimped subfibrils, arranged in parallel at each sublevel; the waviness at each level is treated as a random variable;
- all the random variables are considered as stochastically independent;
- no compressive or bending stiffness is considered;
- the tropocollagen molecules are seen as forming wavy cables, of which the stress-carrying ones are treated as continuous, running from end to end of the bundle, and having an elastic-brittle behaviour.

*New features:*

- a bilinear elastic law is adopted for the tropocollagen molecule, as suggested in [Buehler and Wong 2007];
- the statistical aspects of the molecular failure are based on a simpler yet more consistent assumption, expressed in terms of displacement instead of force;
- crosslinking is accounted for;
- a beta probability density function is chosen for the statistics of all the random quantities;
- account is taken of the possible coexistence, at any sublevel, of stress-carrying and non-stress-carrying material.

The model herein proposed is valid for any material — and specially for soft tissues or tissue components — whose internal microstructure is made by nested wavy thin cables. Its effectiveness, in the context of collagen, is tested by comparing its predictions with the results of experiments available in the literature for single collagen fibres. An indirect verification is also presented, obtained by inserting the new fibre stress-stretch equation into a previously developed model for the mechanical behaviour in tension of the periodontal ligament (PDL) [Genna 2006].

## 2. Theory: the constitutive model

Figure 1 shows a sketch of the assumed hierarchy of subcomponents inside a collagen fibre, based on the description presented, for instance, in [Kastelic et al. 1978]. This follows [AG]; Figure 1 also shows the approximate geometrical scales of each level. The nomenclature adopted here is the following:

- Collagen fibre (or bundle, or fascicle): this is called here “level 0”, and it is the component for which we desire to obtain a stress-stretch equation, starting from its uncoiled, unstretched configuration. Its characteristic diameter is, for collagen types I, II, and III, of about  $100\ \mu\text{m}$ . The uncoiled, unstretched length of the fibre, inside the proposed model, is taken as deterministic, denoted by  $L_b$ .
- Fibril: this is called here “level 1”, and has a typical diameter of about 10 to 500 nm. This component exhibits a typical banded structure, with a period of about 65 nm, that derives from the features of the molecular arrangement [Petruska and Hodge 1964].
- Subfibril: this is called here “level 2”. According to [Kastelic et al. 1978], this entity, of diameter ranging from 10 to 20 nm, has been described in previous literature; it seems hard to be distinguished from the next one (see also [AG]).
- Microfibril, formed by five tropocollagen units joined together: this is called here “level 3”, and has a typical diameter of 3.5 nm;
- Tropocollagen molecule, having a diameter of 1.5 nm: this is the lowest level considered here, i.e., “level 4”.

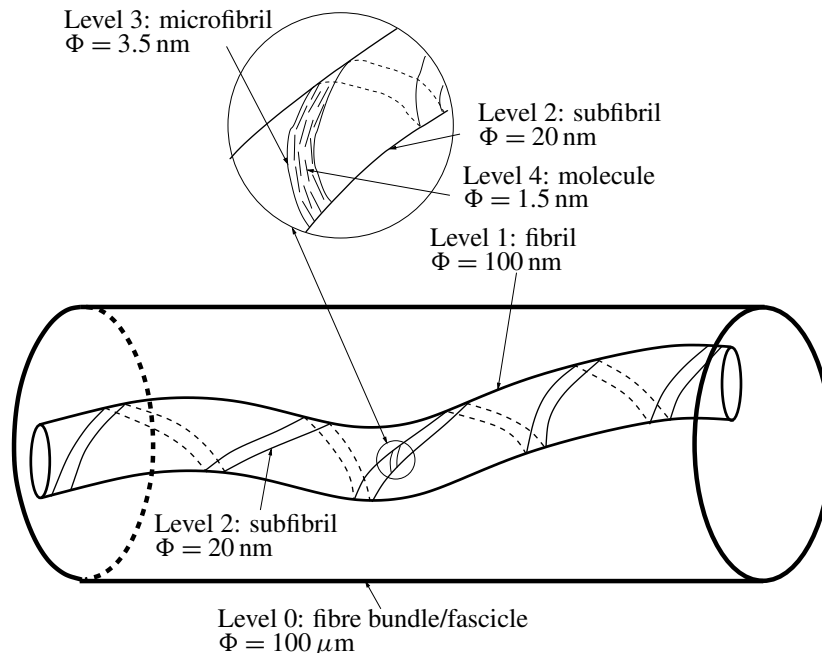


**Figure 1.** Schematic representation of the internal structure of a fibre-forming collagen fibre, as proposed for instance in [Kastelic et al. 1978].

---

**List of abbreviations**

$A_m$	Molecular cross-section area	1.7671 nm <sup>2</sup>
$f_i$	Volume fraction of fibrous matter in cable $i$	
$F_s$	Molecular force at the end of stiffness stage 2	
$F_m$	Molecular force	
$F_{4,A}$	Force in cable 4 during molecular stiffness stage 2	
$F_{4,B}$	Force in cable 4 during molecular stiffness stage 3	
$K_s$	Molecular stiffness in molecular stiffness stage 2	10 pN/nm
$K_m$	Molecular stiffness in molecular stiffness stage 3	30 pN/nm
$L_{0,i}$	Coiled end-to-end distance of a cable at level $i$	Random
$L_{0,m}$	Coiled end-to-end distance of a single molecule	Random
$L_b$	Unstretched uncoiled length of a collagen fibre	
$L_{d,i}$	Unstretched uncoiled length of a cable at level $i$	Random
$L_m$	Unstretched uncoiled length of a single molecule	301.7 (204.9) nm
$M$	Number of molecules in cable at level 4	Random
$N$	Total number of levels (cables) in the cable microstructure	4 for a fibre of collagen type I, II, and III
$s$	Molecular displacement range spanned by stiffness stage 2	
$u_1$	Deterministic value of the displacement that stretches a collagen fibre	
$u_f$	Failure molecular displacement	Random
$u_f^*$	Difference between failure molecular displacement and displacement at the end of the first (entropic) stiffness stage	
$u_i$	Displacement of cable at level $i$ starting from situation when cable $i-1$ is uncoiled and unstretched	
$\bar{u}_i$	Displacement $u_i$ corresponding to complete uncoiling, but with no stretching, of cable at level $i$	
$u_m$	Molecular displacement starting from rest (coiled) configuration	
$\bar{u}_m$	Molecular displacement $u_m$ corresponding to complete uncoiling, but with no stretching, of a single molecule	
$u_s$	Molecular displacement $u_m$ corresponding to the end of stiffness stage 2 of a single molecule	Random
$X_f$	Crosslink parameter affecting molecular failure	
$X_{ks}$	Crosslink parameter affecting the stiffness in molecular stiffness stage 2	
$X_{km}$	Crosslink parameter affecting the stiffness in molecular stiffness stage 3	
$y_i$	Ratio between coiled end-to-end distance and unstretched uncoiled length of cable at level $i$	Random
$z_4$	Product $y_1 y_2 y_3 y_4$	Random
$z_A$	Current value of variable $z_4$ at the beginning of molecular stiffness stage 2 for cable 4	
$z_B$	Current value of variable $z_4$ at the transition between molecular stiffness stages 2 and 3 for cable 4	
$z_C$	Current value of variable $z_4$ at failure for cable 4	
$z_{C,0}$	Value of variable $z_4$ at failure for cable 4 with zero crosslinking	
$\Phi_m$	Molecular diameter	1.5 nm
$\sigma_0$	Cauchy stress in a collagen fibre	Random
$\sigma_i^e$	Stress in the non-fibrous matter in a cable at level $i$	0

---

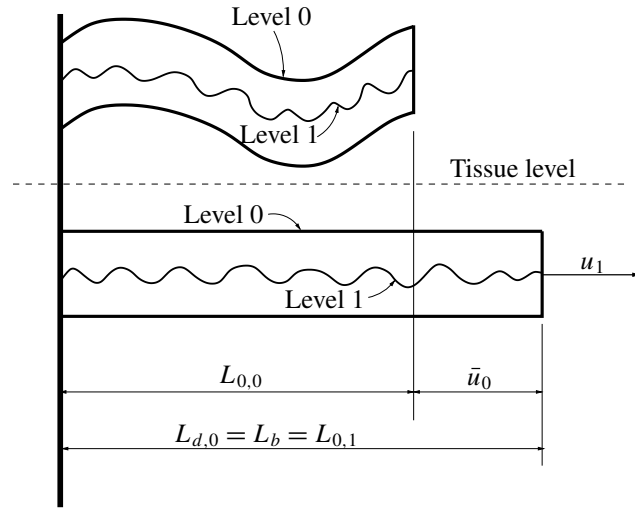


**Figure 2.** Symbols adopted for the top two levels in the assumed hierarchy. Level 0 is the collagen fibre; level 1 is a collagen fibril;  $u_1$  is the deterministic input displacement value, corresponding to actual stretching of the collagen fibre.

In the model presented here, all the stress-carrying subcomponents, at all levels, are assumed to be continuous wavy cables, running from end to end of the collagen fibre. At each level  $i$ , a random number of stress-carrying extensible cables exist, with a wavy/crimped geometry. They are characterised by their uncoiled, unstretched length  $L_{d,i}$ , and by their coiled end-to-end distance, denoted by  $L_{0,i}$ , never longer than  $L_{d,i}$ . Both  $L_{d,i}$  and  $L_{0,i}$  are defined in an undeformed configuration, taken at the instant when the upper level,  $i - 1$ , is fully uncoiled but unstretched. Figure 2 shows the geometry assumed for the first two levels, 0 and 1, defined above. A list of all the symbols adopted in the rest of this work is provided on the previous page for convenience.

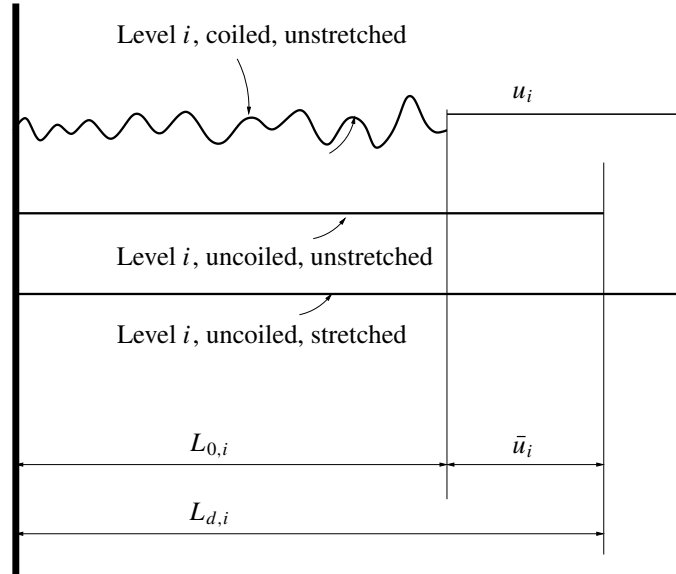
The constitutive equation derived here concerns level 0, starting from the instant at which, upon a prescribed fibre displacement, the fibre has become completely uncoiled. What happens before must be described at the tissue level, since it concerns geometrical properties of the collagen fibre itself. Therefore, the displacement of interest here, taken as the main input data of deterministic value, is the one denoted as  $u_1$  in Figure 2, i.e., the displacement that causes an actual stretch in the collagen fibre. We assume that if  $u_1 \leq 0$ , no stress exists in the fibre.

Figure 3 shows the geometrical features of the considered problem at a generic level  $i$ . At each level, the subfibril displacement  $u_i$  is defined starting from the coiled, unstretched configuration with end-to-end distance  $L_{0,i}$ . For each level  $i$  one has

$$L_{d,i} = L_{0,i+1}, \quad i = 0, \dots, N - 1, \tag{1}$$

where  $N$  indicates the total number of sublevels in the considered microstructure; for a collagen fibre,  $N$  will always be set equal to 4. Equation (1) implies, as shown in Figure 2, that the deterministic input length  $L_b$  corresponds to

$$L_b = L_{d,0} = L_{0,1}. \tag{2}$$



**Figure 3.** Symbols adopted for a generic internal level of the assumed microstructure.

The displacement  $u_i$  contains a part that uncoils the subcomponent  $i$  without stretching it: this part is denoted by  $\bar{u}_i$ , defined as

$$\bar{u}_i = L_{d,i} - L_{0,i} \geq 0. \quad (3)$$

For each level  $i$ , the following nondimensional quantity is defined:

$$y_i = \frac{L_{0,i}}{L_{d,i}}, \quad 0 < y_i \leq 1, \quad (4)$$

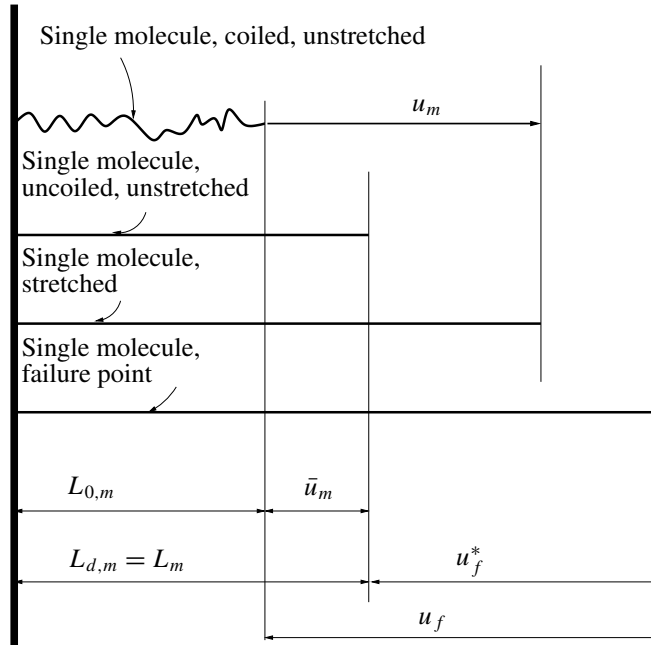
i.e., the ratio between the coiled end-to-end distance and the uncoiled, unstretched length of the subfibrils at that level. The quantities  $y_i$  are assumed to be random variables, governed by a probability density function of the beta type [Ross 2004], because of their taking values in the interval  $[0, 1]$ . It is assumed that (i) the quantities  $y_i$ , for all  $i$ , are stochastically independent, and that (ii) a mean value  $E(y_i)$  and a variance  $\text{Var}(y_i)$  of each  $y_i$  are both known.

Exploiting (1)–(4), and following the same path taken in [AG] (where, though, a different definition of the random variables was adopted), the following results can be obtained:

$$L_{d,i} = \frac{L_b}{\prod_{j=1}^i y_j}, \quad 1 \leq i \leq N, \quad (5)$$

$$u_i - \bar{u}_i = u_1 + L_b \left( 1 - \frac{1}{\prod_{j=1}^i y_j} \right), \quad 1 \leq i \leq N. \quad (6)$$

It is now necessary to define the mechanical behaviour at the tropocollagen molecule level, herein called “level 4”.



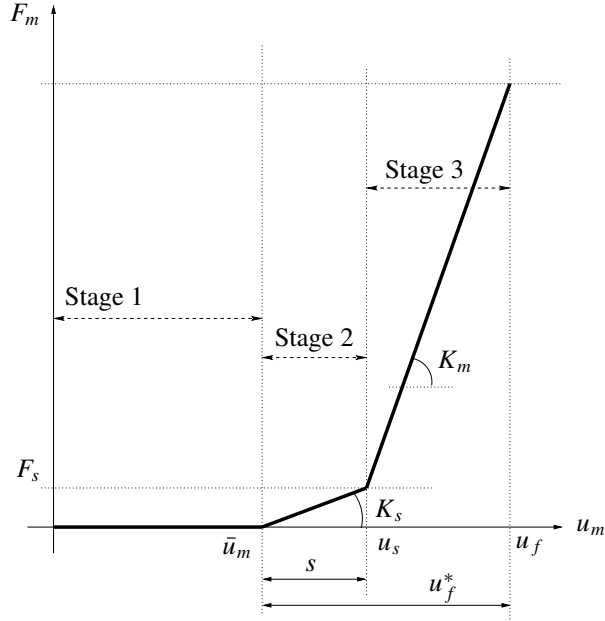
**Figure 4.** Symbols adopted for the displacements of a single tropocollagen molecule. The uncoiled, unstretched length  $L_{d,m}$  of a single molecule coincides with its contour length  $L_m$ .

Figure 4 shows the geometry and the symbology adopted for a *single* molecule. Note that all the symbols previously introduced refer to continuous subcomponents, at all levels, running from end to end of the collagen fibre. In Figure 4, the subscripts  $m$  and  $f$  refer instead to a single molecule, and  $u_m$  is the molecular displacement defined from the coiled, unstretched configuration of a single molecule.

The contour length  $L_m$  is the uncoiled, unstretched length of the molecule, usually (but not always) taken equal to  $L_m = 301.7$  nm (see for instance [Buehler and Wong 2007]). It is the sum of the end-to-end distance of the coiled molecule,  $L_{0,m}$ , with the displacement  $\bar{u}_m$  necessary to fully uncoil the molecule. Both these quantities are assumed to be random variables. The displacement  $u_f^*$  that brings the molecule from its uncoiled state up to the brittle failure point (see for instance [Bozec and Horton 2005] and [Buehler and Wong 2007] for experimental evidence of the aspect of a stress-strain curve in tension of a tropocollagen molecule) is assumed to have a deterministic value; yet, the total failure displacement  $u_f = \bar{u}_m + u_f^*$ , defined as starting from the coiled configuration, is also a random variable.

The mechanical properties of a single molecule are defined on the basis of results presented in [Buehler and Wong 2007], where three stages are recognised in the tensile force-displacement behaviour: a first one, of entropic elasticity, up to an axial force of about 10–15 pN; a second one, corresponding to the uncoiling of the molecule triple helix; and a third stage, where the molecular bonds are stretched, that ends with brittle fracture, at a displacement  $u_f^*$  of about 150 nm.

Here, the first stage is neglected, assuming that, for  $u_m \leq \bar{u}_m$ , the molecular force is zero. Next, a bilinear elastic-brittle force-displacement law is assumed, illustrated in Figure 5. The molecule starts furnishing stiffness when  $u_m > \bar{u}_m$ ; at this instant a second stiffness stage begins, spanning a displacement



**Figure 5.** Bilinear force-displacement law adopted for a single tropocollagen molecule.  $F_m$  is the molecular force;  $u_m$  is the molecular displacement, defined from the initial (coiled) state;  $u_f$  indicates the brittle failure point. Both  $s$  and  $u_f^*$  are assumed to be deterministic quantities. Stage 1 corresponds to entropic elasticity, herein neglected. Stage 2 corresponds to the helix uncoiling phase. Stage 3 corresponds to actual molecular stretching.

range denoted by  $s$ . This stage 2 ends at a displacement  $u_s$  given by

$$u_s = \bar{u}_m + s. \quad (7)$$

During this stage 2, for  $\bar{u}_m \leq u_m \leq u_s$  the molecular stiffness is denoted by  $K_s$ . For  $u_s < u_m \leq u_f$  the molecular behaviour is in a third and final stiffness stage, still linear elastic, but governed by a different stiffness value, indicated by  $K_m$ .

We assume as deterministic, and known, beside the value of  $u_f^* = u_f - \bar{u}_m$ , also (i) the two stiffnesses  $K_s$  and  $K_m$ , and (ii) the displacement interval  $s$  spanning the stiffness stage 2. Also the molecular diameter  $\Phi_m$  is assumed as deterministic and known, of value  $\Phi_m = 1.5$  nm; this value is assumed to remain constant during the deformation.

The assumed force-displacement law for a single tropocollagen molecule is then as follows:

$$\begin{aligned} F_m &= 0, & u_m &\leq \bar{u}_m \text{ (entropic elasticity, neglected);} \\ F_m &= K_s(u_m - \bar{u}_m), & \bar{u}_m &< u_m \leq u_s \text{ (uncoiling);} \\ F_m &= F_s + K_m(u_m - u_s), & u_s &< u_m \leq u_f = (\bar{u}_m + u_f^*) \text{ (stretching);} \\ F_m &= 0, & u_m &> u_f \text{ (failed),} \end{aligned} \quad (8)$$

with

$$F_s = K_s s = K_s (u_s - \bar{u}_m). \tag{9}$$

One needs next to describe the mechanical behaviour of a full cable at the molecular level, assumed to run continuously from end to end of the considered collagen fibre. This subcomponent is made of a series of a number  $M$  of tropocollagen molecules, given by

$$M = \frac{L_{d,4}}{L_m} \gg 1, \tag{10}$$

which, accounting for (5), can also be written as

$$M = \frac{L_b}{L_m \prod_{i=1}^4 y_i} = \frac{L_b}{L_m z_4}, \tag{11}$$

where the new random quantity  $z_4$  was defined as

$$z_4 = \prod_{i=1}^4 y_i, \quad 0 < z_4 \leq 1. \tag{12}$$

In the lack of precise information, it is assumed that the molecules are connected sequentially in a line which, however, has a waviness whose statistical properties are independent from those of a single molecule; furthermore, it is assumed that the polymerisation along the whole collagen fibre is equal to that of the molecule itself, and that both the stiffness and strength of the connection between molecules are the same as those of the molecule itself.

It is now possible to write the force-displacement equations for a single, continuous cable, at level 4, on the basis of the molecular equations (8), because the following hold:

$$u_4 = M u_m, \tag{13}$$

$$\bar{u}_4 = M \bar{u}_m, \tag{14}$$

$$u_4 - \bar{u}_4 = u_1 + L_b \left(1 - \frac{1}{z_4}\right), \tag{15}$$

(see (6)),

$$F_4 = F_m. \tag{16}$$

Hence, denoting by  $F_{4,A}$  and  $F_{4,B}$  the forces in molecular stiffness stages 2 and 3, respectively, one has:

$$F_{4,A} = K_s (u_m - \bar{u}_m) = \frac{K_s}{M} (u_4 - \bar{u}_4) = K_s L_m \left[ \left( \frac{u_1}{L_b} + 1 \right) z_4 - 1 \right], \quad \bar{u}_4 < u_4 \leq u_{s4}, \tag{17}$$

with  $u_{s4} = M u_s$ ;

$$\begin{aligned} F_{4,B} &= F_s + K_m (u_m - u_s) = F_s + \frac{K_m}{M} (u_4 - u_{s4}) \\ &= F_s + K_m L_m \left[ \left( \frac{u_1}{L_b} + 1 \right) z_4 - \left( 1 + \frac{s}{L_m} \right) \right], \quad u_{s4} < u_4 \leq M u_f; \end{aligned} \tag{18}$$

and

$$F_4 = 0, \quad u_4 - \bar{u}_4 \leq 0 \quad \text{or} \quad u_4 - \bar{u}_4 > M u_f^*. \tag{19}$$

From (17) and (18), it becomes apparent that the only random quantity that governs the mechanical behaviour of each cable at level 4 is  $z_4$ , defined by (12). The probability density function of  $z_4$  cannot be defined in closed form, but it is assumed to be also a beta function, with known mean value and variance, that can be computed, for the product of stochastically independent random variables, exploiting the following expressions:

$$\text{if } x = y_i y_j, \quad \text{then } E(x) = E(y_i)E(y_j); \quad (20)$$

$$\text{if } x = y_i y_j, \quad \text{then } \text{Var}(x) = [E(y_i)]^2 \text{Var}(y_j) + [E(y_j)]^2 \text{Var}(y_i) + \text{Var}(y_i) \text{Var}(y_j) \quad (21)$$

(see for instance [Goodman 1960; 1962]).

Denoting now by  $f_{z_4}(z_4)$  the probability density function for  $z_4$ , the expected value of  $F_4$ , for each assigned value of the collagen fibre displacement  $u_1$ , must be computed through an integration over the admissible values of  $z_4$ , as follows:

$$E[F_4(u_1, z_4)] = \int_{0 < z_A \leq 1}^{0 < z_B \leq 1} F_{4,A}(z_4) f_{z_4}(z_4) dz_4 + \int_{0 < z_B \leq 1}^{0 < z_C \leq 1} F_{4,B}(z_4) f_{z_4}(z_4) dz_4 \quad (22)$$

The integration limits  $z_A$ ,  $z_B$ , and  $z_C$ , all deterministic, are to be computed as follows:

- from (15) and (19) one has

$$F_{4,A} \neq 0 \quad \text{if} \quad u_1 + L_b \left(1 - \frac{1}{z_4}\right) > 0 \quad \Rightarrow \quad z_4 > \frac{L_b}{u_1 + L_b} = z_A; \quad (23)$$

- from (17) it is seen that the transition from  $F_{4,A}$  to  $F_{4,B}$  occurs for  $u_4 = u_{s4}$ , i.e., for

$$u_4 = M u_s = \bar{u}_4 + M s, \quad (24)$$

which, recalling (11) and again (15), gives

$$z_B = \frac{L_b}{u_1 + L_b} \left(1 + \frac{s}{L_m}\right); \quad (25)$$

- and from (11), (15), and (18) one has

$$F_{4,B} \neq 0 \quad \text{if} \quad u_1 + L_b \left(1 - \frac{1}{z_4}\right) < \frac{L_b}{L_m z_4} u_f^* \quad \Rightarrow \quad z_4 < \frac{L_b}{u_1 + L_b} \left(1 + \frac{u_f^*}{L_m}\right) = z_C. \quad (26)$$

Note that, in order to account for the irreversibility of failure, in the calculation of integral (22) the upper integration limit  $z_C$  can not increase with increasing  $u_1$ , i.e., one must always set  $dz_C/du_1 \leq 0$ .

It is now possible to introduce into the previous equations some simple modifications in order to account for the possible presence of crosslinking. For this complex aspect, no attempt is made here at describing any physical feature of the substructural arrangement. The purpose is to model the main mechanical effects of crosslinking in a phenomenological way, through equations void of physical meaning, but as simple as possible.

The main effects of crosslinking considered herein are (i) the increase of the apparent stiffness of a single cable (see, for instance, [Thompson and Czernuszka 1995]); (ii) the influence of the brittle failure of a cable on the surrounding ones.

The first effect is described in a trivial way: the basic molecular stiffnesses,  $K_s$  and  $K_m$ , are introduced into the governing equations each multiplied by an independent dimensionless factor, denoted by  $X_{ks} \geq 1$  and  $X_{km} \geq 1$  respectively.

The second effect of crosslinking is recognised to be of reducing the failure displacement of the whole collagen fibre. Such a reduction is quite significant, according to [Pins et al. 1997]: non-crosslinked fibres are reported to fail at a strain (probably Biot, although this is not reported in [Pins et al. 1997]) that can reach values up to 0.68, whereas crosslinked ones fail at strains of the order of 0.15. This phenomenon could be explained considering that brittle failure is associated to a sudden release of elastic energy: if the failed cable is crosslinked to other parallel cables, the surrounding ones might absorb a portion of the released energy, and fail themselves, thus leading to a premature failure of the whole collagen fibre.

This effect has been taken into account by defining a progressive reduction of the upper integration limit in (22), i.e.,  $z_C$  of (26). This reduction is proportional to the current value of the input displacement  $u_1$  through a new nondimensional parameter  $X_f \geq 0$ . We have redefined  $z_C$  as follows:

$$z_C = z_{C,0} - f(X_f, u_1), \quad \frac{dz_C}{du_1} \leq 0, \quad \text{with} \quad z_{C,0} = \frac{L_b}{u_1 + L_b} \left( 1 + \frac{u_f^*}{L_m} \right), \quad (27)$$

and with

$$f(X_f, u_1) = \frac{2 \arctan(u_1 X_f / L_b)(z_{C,0} - z_A)}{\pi}. \quad (28)$$

These equations, which have no physical basis, when inserted into the governing equations allow one to obtain the desired effect: with increasing  $u_1$ , the upper integration limit  $z_C$  tends to approach the lowest one,  $z_A$ . This reflects the progressive disappearance, among the various subcomponents, of the shorter ones, at a rate that increases with increasing values of the parameter  $X_f$ .

The expected value of the axial stress in a cable at level 4, i.e., in a cable made by a sequence of tropocollagen molecules, for a given value of the collagen fibre displacement  $u_1$ , is then

$$E(\sigma_4) = \frac{E(F_4)}{A_m} = \frac{4E(F_4)}{\pi \Phi_m^2}. \quad (29)$$

Elementary homogenisation theory is finally exploited to compute the corresponding expected value of the macroscopic axial stress in the collagen fibre at level 0 of the assumed hierarchy, as shown in Figure 1. At each level, in fact, the stress-carrying subfibrils coexist with noncontinuous subfibrils, with some extra-fibrous (ground) matter, and with no matter at all.

Denote by  $\sigma_i^e$  the tensile stress possibly transmitted by the nonfibrous matter at each level  $i$ , and by  $f_i$  the volume fraction of stress-carrying fibrous matter at each level  $i$ . Then  $f_i = A_i^f / A_i$ , where  $A_i$  is the total area of a cable at level  $i$ , and  $A_i^f$  is the area occupied by continuous fibrous matter in that very cable. Then the elementary homogenisation theory allows one to calculate the average macroscopic stress  $\sigma_0$  at level 0 as follows:

$$\sigma_0 = E(\sigma_4) f_3 f_2 f_1 f_0 + \sigma_3^e (1 - f_3) f_2 f_1 f_0 + \sigma_2^e (1 - f_2) f_1 f_0 + \sigma_1^e (1 - f_1) f_0 + \sigma_0^e (1 - f_0). \quad (30)$$

From now on, for simplicity, we always assume that the extra-fibrous matter does not carry any mechanical stress in tension, even though it could do so in compression. Therefore, we will set  $\sigma_i^e = 0$  for each

$i = 0, \dots, 3$  in (30), which then reduces to

$$\sigma_0 = E(\sigma_4) f_3 f_2 f_1 f_0, \quad (31)$$

with  $E(\sigma_4)$  given by (29), with (22) and following. This is an explicit expression for the axial stress in a single stretched collagen fibre for any corresponding value of the prescribed value of  $u_1$ ; this last could be related to any conventional strain value through standard theory.

We note, finally, that the obtained stress-stretch equation, here derived explicitly for the case of  $N = 4$ , could be easily extended to any other structural component, biological or not, having the same type of microstructure of nested wavy cables, with any number  $N$  of subcomponents. Once the mechanical properties of the most microscopic level — i.e., level  $N$  — are known, a straightforward extension of the above equations will furnish the desired stress-stretch relationship. The only statistics to be described would be that of a variable  $z_N$ , defined as the product of the  $N$  random variables  $y_i$ , defined by (4). The expression for the average macroscopic stress that extends result (30) to an arbitrary number  $N$  of sublevels is the following:

$$\sigma_0 = E(\sigma_N) \prod_{i=0}^{N-1} f_i + \sum_{i=0}^{N-1} \left[ \sigma_i^e (1 - f_i) \prod_{j=0}^{i-1} f_j \right]. \quad (32)$$

The proposed stress-stretch equation, with the force-displacement law of (17) and (18), and with the modifications of (27) and (28), included to account for crosslinking, requires a total number of constitutive parameters equal to  $7 + 3N$  in general, and equal to 19 for the case  $N = 4$ .

### 3. Applicative examples

**3.1. Sea cucumber collagen fibril, from** [Eppell et al. 2006]. The first example considers a collagen fibril, i.e., the subcomponent at level 1 of the hierarchy considered so far. Therefore, to obtain the corresponding results one must adopt  $N = 3$ , and the molecular level corresponds now to  $i = 3$  in (5) and (6). This example was chosen both because it helps in setting a basis for the data concerning the statistics at the lower levels of a fibre, and because there are experimental results available [loc. cit.].

Figure 6 shows tensile stress-strain curves: one as presented in [loc. cit.] (continuous), the other (with white circles) as obtained from the analytical approach proposed here. In this case, unlike all the remaining ones, the molecular length  $L_m$  has been set equal to  $L_m = 204.9$  nm, instead of the commonly adopted value  $L_m = 301.7$  nm, following the results presented in [loc. cit.]. We note (we will return to this in the next section) that a substantial uncertainty about experimentally measured quantities exists already for the “simple” molecular length  $L_m$ . The Almansi strain employed for the abscissa, as done in [loc. cit.], is defined as

$$\varepsilon_{\text{Almansi}} = \frac{\lambda^2 - 1}{2\lambda^2}, \quad \lambda = \frac{L_b + u_1}{L_b}. \quad (33)$$

Table 1 shows the set of parameters adopted to obtain the analytical results for this and the next three examples. The first ten parameters have values that will remain fixed in all the presented examples; the remaining nine will have different values for each example. Note that, for (31), we have not defined individual values for the stress-carrying fibrous matter volume fractions  $f_i$ , but rather a single value for

Material parameter	Sea cucumber fibril [Eppell et al. 2006]	Engineered [Gentleman et al. 2003]	Rat tail [Gentleman et al. 2003]	Rabbit patellar tendon [Yamamoto et al. 1999]
$E(y_2)$	0.9952	0.9952	0.9952	0.9952
$E(y_3)$	0.99779	0.99779	0.99779	0.99779
$E(y_4)$	0.9979	0.9979	0.9979	0.9979
$\text{Var}(y_2)$	$4.9 \cdot 10^{-5}$	$4.9 \cdot 10^{-5}$	$4.9 \cdot 10^{-5}$	$4.9 \cdot 10^{-5}$
$\text{Var}(y_3)$	$6.561 \cdot 10^{-7}$	$6.561 \cdot 10^{-7}$	$6.561 \cdot 10^{-7}$	$6.561 \cdot 10^{-7}$
$\text{Var}(y_4)$	$2.5027 \cdot 10^{-6}$	$2.5027 \cdot 10^{-6}$	$2.5027 \cdot 10^{-6}$	$2.5027 \cdot 10^{-6}$
$\prod f_i$	0.0768	0.05	0.05	0.05
$K_s$ (pN/nm)	10	10	10	10
$K_m$ (pN/nm)	30	30	30	30
$\Phi_m$ (nm)	1.5	1.5	1.5	1.5
$L_m$ (nm)	204.9	301.7	301.7	204.9/301.7
$u_f^*$ (nm)	265	167	167	75
$E(y_1)$	-	0.99	0.99	0.99
$\text{Var}(y_1)$	-	$1.7742 \cdot 10^{-4}$	$1.7742 \cdot 10^{-4}$	$8.281 \cdot 10^{-5}$
$L_b$ (mm)	5	76	76	15
$X_{ks}$	1.8	3.64	15	6.5
$X_{km}$	5	2.25	2	1
$X_f$	0.12	9.85	6.8	15
$s$ (nm)	115	23	32	5

**Table 1.** Values adopted for the material parameters of the collagen fibril and collagen fibres.

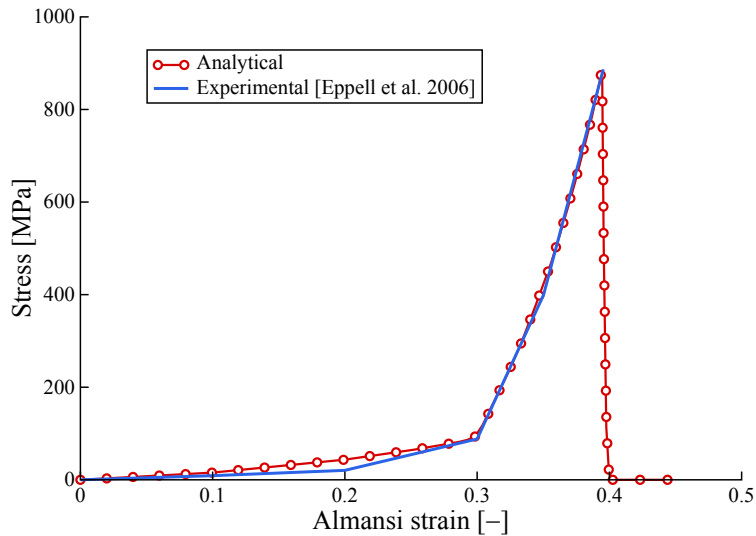


**Figure 6.** Stress-strain curves in uniaxial tension for the collagen fibril studied in [Eppell et al. 2006]. The blue curve is experimental [loc. cit.]; the red curve is obtained from the proposed equations. The Almansi strain is defined as in (33). Material data as in Table 1.

their product, based on the considerations presented in Section 4. A good agreement between experimental and analytical results could be found for this special example. The analytical result provides the expected value for the fibril stress; for this example, the peak stress expected value is 884 MPa, to which a predicted standard deviation of 4157 MPa corresponds.

**3.2. Engineered collagen fibre, from** [Gentleman et al. 2003]. The next example concerns the engineered collagen fibre studied in [loc. cit.]. Figure 7 shows tensile stress-strain curves: one as presented in [loc. cit.], and the others as obtained from the proposed analytical approach. The Biot strain in the abscissa — the same adopted in [loc. cit.] — is defined as

$$\varepsilon_{\text{Biot}} = \frac{u_1}{L_b}. \quad (34)$$

A good agreement between experimental results and analytical predictions can be observed. In this case, the peak stress expected value is 70.8 MPa, and the corresponding standard deviation is 419.5 MPa.

The other curves, with white markers, refer to analytical results obtained from different choices of material parameters, in order to provide a brief sensitivity analysis: each curve refers to the modification of a single parameter, with respect to those listed in Table 1. The following effects, easy to predict on the basis of the meaning of the considered parameters, are visible:

- a reduction of the molecular failure displacement,  $u_f^*$ , causes a reduction of both the global peak stress and strain, leaving the overall shape of the stress-strain curve unaltered;
- a reduction of the size of stage 2 of the molecular stiffness, through parameter  $s$  (see Figure 5), causes a corresponding increase of the overall stiffness, as well as of the global peak stress;

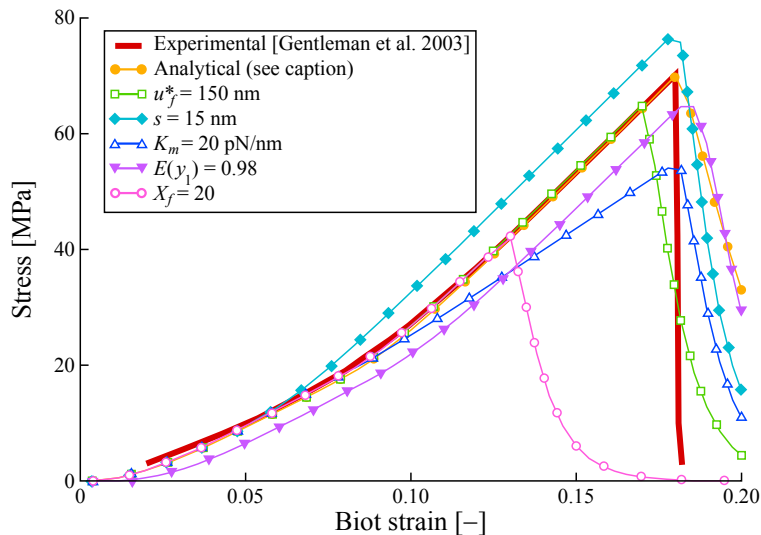


**Figure 7.** Stress-strain curves in uniaxial tension for the engineered collagen fibre studied in [Gentleman et al. 2003]. The solid curve is experimental, from [loc. cit.]; all the other curves, with markers, are obtained from the proposed equations. The Biot strain is defined in (34). Material data as in Table 1.

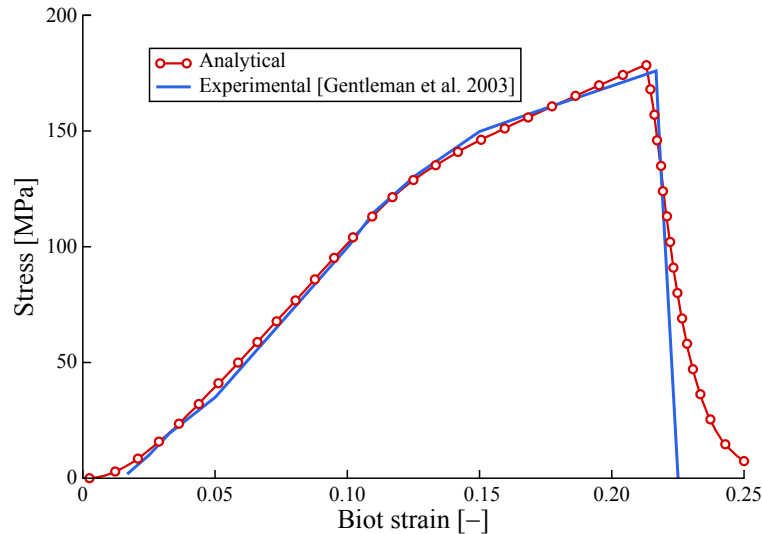


**Figure 8.** Stress-strain curves in uniaxial tension for the rat tail collagen fibre studied in [Gentleman et al. 2003]. The solid curve is experimental, from [loc. cit.]; the curve with circles is obtained from the proposed equations. Material data as in Table 1.

- a reduction of the molecular stiffness  $K_m$  has the opposite effect;
- a reduction of the expected value for the variable  $y_1$  of (4) causes a change of shape of the stress-strain curve, as well as a reduction of the peak stress for the fibre;
- an increase of the parameter  $X_f$  causes a significant loss of ductility, as expected.

The model is relatively insensitive to small variations of the variances for the single variables  $y_i$  of (4).

**3.3. Rat tail tendon collagen fibre, from** [Gentleman et al. 2003]. Figure 8 shows a similar comparison, concerning now a single collagen fibre extracted from a rat tail tendon, as reported in [loc. cit.]. In this case, the peak stress expected value is 178.7 MPa, and the corresponding standard deviation is 1049 MPa.

**3.4. Rabbit patellar tendon sample, from** [Yamamoto et al. 1999]. Figure 9 illustrates results similar to the previous ones for a collagen fibre taken from a rabbit patellar tendon, for which experimental results are provided in [loc. cit.]. The figure shows two analytical curves, of which only the one adopting  $L_m = 204.9$  nm, as done for the fibril example, corresponds well to the experimental result. In this case, the peak nominal stress (nominal stresses are shown in [loc. cit.]) expected value is 19.62 MPa, and the corresponding standard deviation is 116 MPa.

**3.5. Periodontal ligament sample, from** [Genna et al. 2008]. Figure 10 shows again a stress-strain plot, that now concerns the behaviour in tension of a small sample of swine periodontal ligament (PDL). The details of the sample and of the testing modalities are described in [loc. cit.]. In this case, the experiment concerns a tissue, not a single collagen fibre, and one has only an indirect validation of the model proposed herein.

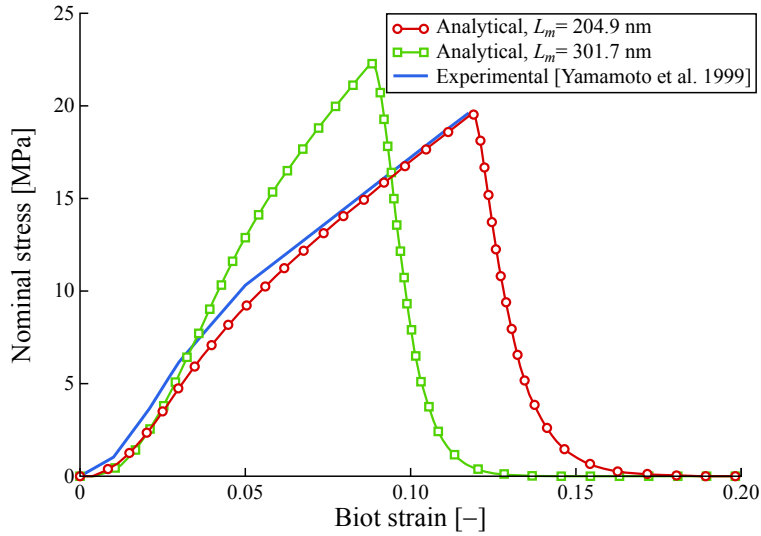


**Figure 9.** Stress-strain curves in uniaxial tension for the rabbit patellar collagen fibre studied in [Yamamoto et al. 1999]. The solid curve is experimental, from [loc. cit.]; the curves with markers are obtained from the proposed equations, and refer to different molecular lengths  $L_m$  as indicated. The nominal stress is force divided by initial cross-section area. Material data as in Table 1.

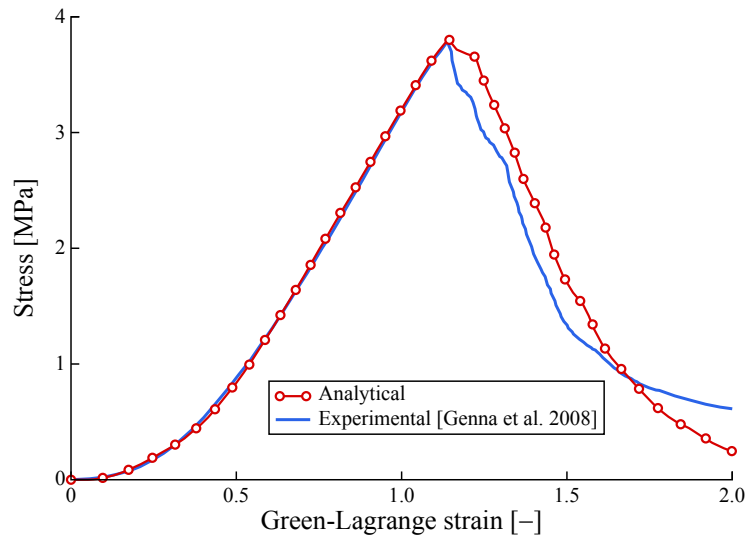


**Figure 10.** Stress-strain curves in uniaxial tension for one of the periodontal ligament samples studied in [Genna et al. 2008]. The solid curve is experimental, from [loc. cit.]; the curve with circles is obtained by means of the model of [Genna 2006], in which the equations developed in the present work have been inserted for the behaviour in tension of a single collagen fibre. The Green-Lagrange strain is defined as in (35) of the text. Material data as in Table 2.

The Green–Lagrange strain plotted in abscissa in Figure 10, as adopted in [loc. cit.], is defined as

$$\varepsilon_{GL} = \frac{1}{2} \left[ \left( \frac{L_b + u_1}{L_b} \right)^2 - 1 \right]. \tag{35}$$

In this case, (31) is inserted into an interface model, presented in [Genna 2006], that allows one, by means of yet another statistical integration over the waviness of the collagen fibres, to describe the tissue features. The accompanying paper [Genna and Paganelli 2014] makes extensive use of this model for studying the extraction of a tooth from its socket; we refer to [Genna 2006] and [Genna and Paganelli 2014] for more details of the interface description.

The main parameters required by the PDL model of [Genna 2006] are:

- the thickness  $w_0$  of the PDL layer;
- the angle  $\beta_0$  that defines the inclination of the collagen fibres in a longitudinal section of the tooth;
- the angle  $\theta_0$  that defines the inclination of the collagen fibres in a transversal section of the tooth;
- the volume fraction  $f_c$  of stress-carrying collagen fibres inside the PDL;
- statistical properties of the collagen fibres waviness in the PDL, described by the variable  $x_c$  which is the ratio between the uncoiled, unstretched length of a collagen fibre and its end-to-end distance at rest, governed by  $w_0$ ,  $\beta_0$ , and  $\theta_0$ ;
- data for the constitutive law of a single collagen fibre, that here correspond to the 19 parameters required by the proposed stress-stretch model;
- other parameters that define the compressive behaviour of the PDL, of no interest here.

Table 2 reports all the relevant data adopted to obtain the result shown in Figure 10. In Table 2 the parameter  $L_b$ , denoting the uncoiled length of a collagen fibre at rest, is marked as a random variable, since its value now depends on the statistics of the waviness of the fibre, i.e., on the current values of  $x_c$  during the integration process.

$E(y_2)$	0.9952	$u_f^*$	167 nm	$w_0$	0.66 mm
$E(y_3)$	0.99779	$E(y_1)$	0.995	$\beta_0$	34°
$E(y_4)$	0.9979	$\text{Var}(y_1)$	$1.2078 \cdot 10^{-4}$	$\theta_0$	76.8°
$\text{Var}(y_2)$	$4.9 \cdot 10^{-5}$	$L_b$	random variable	$f_c$	0.05
$\text{Var}(y_3)$	$6.561 \cdot 10^{-7}$	$X_{ks}$	1	$E(x_c)$	1.093
$\text{Var}(y_4)$	$2.5027 \cdot 10^{-6}$	$X_{km}$	1	$\text{Var}(x_c)$	0.00397
$f_0 f_1 f_2 f_3$	0.05	$X_f$	0		
$K_s$	10 pN/nm	$s$	50 nm		
$K_m$	30 pN/nm				
$\Phi_m$	1.5 nm				
$L_m$	301.7 nm				

**Table 2.** Adopted values for the material parameters of the periodontal ligament sample studied in [Genna et al. 2008].

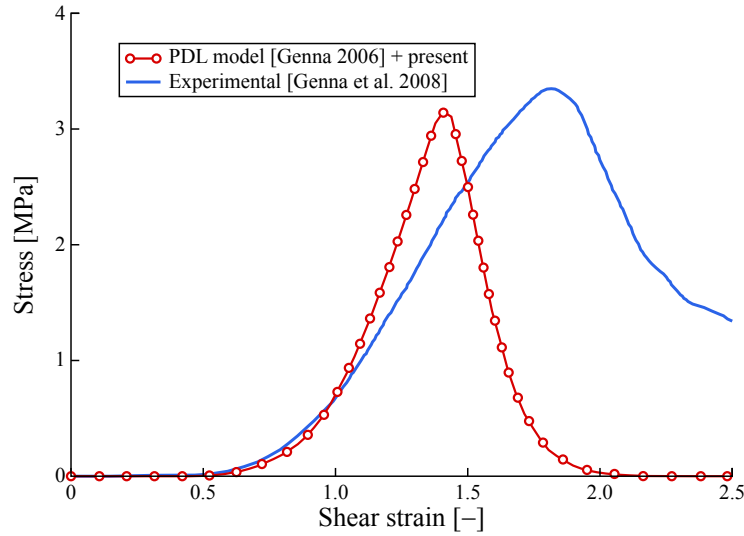


**Figure 11.** Stress-strain curves in shear for one of the periodontal ligament samples studied in [Genna et al. 2008]. The solid curve is experimental, from [loc. cit.]; the curve with circles is obtained by means of the model of [Genna 2006], in which the equations developed in the present work have been inserted for the behaviour in tension of a single collagen fibre. The shear strain is defined as the ratio between the displacement and the width at rest of the sample. Material data as in Table 2 except for  $w_0 = 0.33$  mm and  $\beta_0 = -7^\circ$ .

It is worth remarking, here, that the failure Biot strain of a single collagen fibre, with the data adopted to obtain the result of Figure 10, is  $\varepsilon_f \approx 0.55$ . As already observed, this quite large value is an indication of the probable lack of crosslinking in the PDL collagen.

Finally, Figure 11 shows a comparison obtained in the same way as the previous one, but on a different swine PDL sample, and for a different type of loading, i.e., shear in a plane normal to the tooth axis [Genna et al. 2008]. The curves in Figure 11 show a shear stress in ordinate, and, in abscissa, a shear strain defined as the ratio between the shear displacement and the width  $w_0$  of the PDL sample. For this case the adopted data are the same as in Table 2, with the exception of  $w_0$  and  $\beta_0$ , which are now  $w_0 = 0.33$  mm and  $\beta_0 = -7^\circ$ .

#### 4. Discussion

A main source of difficulty for the model proposed here is the choice of the material parameter values. Results of a detailed sensitivity analysis, beside what was shown in Figures 7 and 9, are not reported here for the sake of brevity.

All the data concerning the statistics of the quantities  $y_i$  of (4), shown in Tables 1 and 2, have been rederived following the same approach adopted in [AG]. A partial confirmation of their usability derives from the result shown in Figure 6, which refers to a subcomponent of the fibres.

A precise evaluation of the volume fractions  $f_i$  of stress-carrying cables at the various sublevels can hardly be given. The following approach was therefore followed: a single cable at level  $i$  is assumed to

have a circular cross-section; fibrous matter is assumed to be present in cables, at level  $i + 1$ , also having a circular cross-section. For a full packing of infinite equal circles, the volume fraction of fibrous matter would be equal to  $\pi/\sqrt{12} \approx 0.907$ , at each sublevel. Assuming a large but finite number of internal circles, one can adopt a smaller value, that we chose equal to 0.85. Furthermore, it was necessary to define what part of the fibrous subcomponents, at each level, was continuous, i.e., stress-carrying: we assumed that only one half of the fibrous matter was continuous, thus obtaining a value  $f_i \approx 0.425$ . Therefore, one finds  $f_0 f_1 f_2 f_3 \approx 0.425^4 = 0.033$ , rounded to  $f_0 f_1 f_2 f_3 = 0.05$ , and  $f_1 f_2 f_3 = 0.0768$  for the fibril, with  $N = 3$ , as shown in Tables 1 and 2.

More difficulties arise in defining several molecular parameters. We started by reasoning on the case of the periodontal ligament (PDL), in order to exclude the effects of crosslinking: in this tissue, in fact, the stress-carrying fibres seem to behave as if little or no crosslinking at all were present. This could be inferred from (i) the very low stiffness values, and the very large failure strains, compared to other tissues, observed in PDL samples [AG], and (ii) as said in Section 3.3, from the high value of the single fibre failure strain. No quantitative description of this aspect could be found; [Berkovitz et al. 1995] reports that PDL has “unique” crosslinking features, with respect to all other tissues, but no information is given about the relevance of this property with respect to mechanical behaviour.

Thus, the stress-carrying collagen fibres of the PDL were assumed to be uncrosslinked. This implies, in the approach illustrated here, to adopt  $X_{ks} = X_{km} = 1$  and  $X_f = 0$ , which allows one to reason about raw molecular data.

In order to obtain a good match with the experimental result in tension of Figure 10, the values  $K_s = 10$  pN/nm,  $K_m = 30$  pN/nm,  $u_f^* = 167$  nm, and  $s = 50$  nm were adopted (see Table 2).

The displacement values agree reasonably well with the corresponding ones reported in [Buehler and Wong 2007], which are  $u_f^* = 150$  nm and  $s = 90$  nm. On the contrary, the molecular stiffness ones do not, since our  $K_m$  is ten times smaller than the one obtained in [Buehler and Wong 2007], and  $K_s$  is about 1/5. It is extremely difficult to obtain coherent information about these data from the literature, for several reasons. A relationship exists that relates the bending stiffness of a tropocollagen molecule to its persistence length, but this seems to hold for the entropic regime only, neglected here. Another relationship which provides the molecular stiffness in the stretching range derives from standard truss theory, and is

$$K_m = \frac{E_m A_m}{L_m}, \quad (36)$$

where  $E_m$  denotes the molecule Young modulus. According to several sources (see, for instance, [Gautieri et al. 2012]), the Young modulus of a collagen molecule takes values in the range  $E_m = 300$ – $16000$  pN/nm<sup>2</sup> (i.e., MPa), depending both on the evaluation modalities and on the considered strain rate, both in experiments and in numerical simulations based on molecular dynamics theory.

Adopting an average value  $E_m = 5000$  pN/nm<sup>2</sup>, equation (36) yields  $K_m = 29.98$  pN/nm. On the other hand, a value  $E_m = 5000$  pN/nm<sup>2</sup> hardly agrees with further data reported in [Buehler and Wong 2007], where the bending stiffness of a single molecule is reported to vary between  $E_m I_m = 1.247 \times 10^{-29}$  Nm<sup>2</sup> and  $E_m I_m = 1.2 \times 10^{-28}$  Nm<sup>2</sup>, depending on the assumed strain rate,  $I_m$  denoting the molecule moment of inertia around its neutral axis. Assuming for the molecule a circular cross-section with diameter  $\Phi_m = 1.5$  nm, the first value corresponds to  $E_m \approx 50$  pN/nm<sup>2</sup>, and the second to  $E_m \approx 500$  pN/nm<sup>2</sup>.

On yet another hand, in order to obtain the stiffness value  $K_m = 294.8$  pN/nm proposed in [Buehler and Wong 2007] for the molecular stretching regime, (36) would require a value  $E_m \approx 50000$  pN/nm<sup>2</sup>, well outside the reported range of values. This uncertainty on the value of  $K_m$  may arise from the intrinsic measurement difficulties, from confusion between entropic and energetic behaviour, from presence/absence of crosslinking, strain-rate effects, solvated/dry conditions during the test, and so on.

In order to obtain results from the stress-stretch model proposed in this work, it was arbitrarily decided to assume as valid the average value  $E_m = 5000$  pN/nm<sup>2</sup>, which corresponds to  $K_m \approx 30$  pN/nm, for the uncrosslinked, basic molecular stiffness. All the choices for the molecular parameters are made very difficult by the lack of reliable experimental results; even the basic molecular length  $L_m$  does not see agreement on its values (here we have been forced to adopt the values  $L_m = 204.9$  nm or  $L_m = 301.7$  nm in different cases.)

As for  $K_s$ , the molecular stiffness associated to the chain uncoiling, the situation is even less clear than for  $K_m$ . Its value could only be identified, and it was taken equal to  $K_s = 10$  pN/nm, in a proportion to  $K_m$  about twice as that indicated in [Buehler and Wong 2007].

The numerical values of the three parameters  $X_{ks}$ ,  $X_{km}$ , and  $X_f$ , that govern crosslinking, in the results of Figures 7, 8, and 9, had to be identified case by case.

As for the last rows in Table 2, that concern the data defining the PDL behaviour, we refer to [Genna 2006], except for  $f_c$  of Section 3.3. In [loc. cit.] every single collagen fibre was supposed to run continuously from end to end of the PDL layer, and the value for the fibre volume fraction  $f_c$  was taken from the literature as equal to  $f_c = 0.5$ . Recent work [Trombetta and Bradshaw 2010] confirms that  $f_c = 0.5$  is a reasonable estimate of the average value for the volume fraction of the fibrous component in the PDL. In the new model, only the stress-carrying portion of it is considered, which, at least according to available images of the PDL, is only a small fraction of the total. In order to obtain a good match with the experimental stress-strain results, the value  $f_c = 0.05$  had to be adopted, as shown in Table 2.

An uncertainty remains about the shape of the stress-strain curves of both Figures 8 and 9, and the relevant material data, shown in Table 1. Work by Gutzmann et al. [2004] suggests that a plateau in the stress-strain curve of collagen might be due to crosslinking; the model proposed here might reproduce this effect through the reduction of the upper integration limit  $z_C$  ((27) and (28)), for increasing displacement  $u_1$ , until the stiffer portion of the molecular behaviour disappears from the picture. Nevertheless, with the set of material parameters herein adopted, and especially in view of the narrow extension of the molecular force-displacement law covered by the statistics of the variable  $z_4$  of (12), it was impossible to obtain such an effect automatically. The only way to reproduce it was to adopt  $X_{ks}K_s < X_{km}K_m$  as shown by Table 1, whose meaning remains unclear.

The simplicity of the model proposed herein allows one to consider any type of mechanical behaviour at the lowermost level — for instance, viscosity — with no conceptual difficulty.

Other considerations, similar to those already reported in [AG], remain still valid also for this modified, simplified, and improved version of the same approach.

## 5. Conclusions

No attempt has been made, here, to propose a complete and accurate representation of the physical microstructure of a single collagen fibre. The aim has been to obtain a simple and engineering-usable

(for instance, in large-scale 3D finite element calculations) set of equations that describe the nonlinear mechanical behaviour of this important biological component, based on a set of parameters having, where possible, a clear physical meaning. Several features of the real arrangement of subcomponents are explicitly taken into account, but several other important details still require more study. The ability to reproduce experimental results on the basis of reasonable values of the material parameters is however encouraging. An accompanying paper [Genna and Paganelli 2014] illustrates the performance of the model presented herein in the context of finite element simulations at the macroscopic scale.

### References

- [Annovazzi and Genna 2010] L. Annovazzi and F. Genna, “An engineering, multiscale constitutive model for fiber-forming collagen in tension”, *J. Biomed. Mater. Res. A* **92A**:1 (2010), 254–266.
- [Berkovitz et al. 1995] B. K. B. Berkovitz, B. J. Moxham, and H. N. Newman, *The periodontal ligament in health and disease*, 2nd ed., Mosby-Wolfe, London, 1995.
- [Bozec and Horton 2005] L. Bozec and M. Horton, “Topography and mechanical properties of single molecule of type I collagen using atomic force microscopy”, *Biophys. J.* **88**:6 (2005), 4223–4231.
- [Buehler and Wong 2007] M. J. Buehler and S. Y. Wong, “Entropic elasticity controls nanomechanics of single tropocollagen molecule”, *Biophys. J.* **93**:1 (2007), 37–43.
- [Bustamante et al. 2000] C. Bustamante, S. B. Smith, J. Liphardt, and D. Smith, “Single-molecule studies of DNA mechanics”, *Curr. Opin. Struct. Biol.* **10**:3 (2000), 279–285.
- [Cacho et al. 2007] F. Cacho, P. J. Elbischger, J. F. Rodriguez, M. Doblaré, and G. A. Holzapfel, “A constitutive model for fibrous tissues considering collagen fiber crimp”, *Int. J. Non-Linear Mech.* **42**:2 (2007), 391–402.
- [Eppell et al. 2006] S. J. Eppell, B. N. Smith, H. Kahn, and R. Ballarini, “Nano measurements with micro-devices: Mechanical properties of hydrated collagen fibrils”, *J. R. Soc. Interface* **3**:6 (2006), 117–121.
- [Gautieri et al. 2012] A. Gautieri, S. Vesentini, A. Redaelli, and M. Buehler, “Viscoelastic properties of model segments of collagen molecules”, *Matrix Biol.* **31**:2 (2012), 141–149.
- [Genna 2006] F. Genna, “A micromechanically-based, three-dimensional interface finite element for the modelling of the periodontal ligament”, *Comput. Methods Biomech. Biomed. Engin.* **9**:4 (2006), 243–256.
- [Genna and Paganelli 2014] F. Genna and C. Paganelli, “Force–displacement relationship in the extraction of a porcine tooth from its socket: Experiments and numerical simulations”, *J. Mech. Mater. Struct.* **9**:5 (2014), 497–514.
- [Genna et al. 2008] F. Genna, L. Annovazzi, C. Bonesi, P. Fogazzi, and C. Paganelli, “On the experimental determination of some mechanical properties of porcine periodontal ligament”, *Meccanica* **43**:1 (2008), 55–73.
- [Gentleman et al. 2003] E. Gentleman, A. Lay, D. Dickerson, E. Nauman, G. Livesay, and K. Dee, “Mechanical characterization of collagen fibers and scaffolds for tissue engineering”, *Biomater.* **24**:21 (2003), 3805–3813.
- [Goodman 1960] L. A. Goodman, “On the exact variance of products”, *J. Amer. Stat. Assoc.* **55**:292 (1960), 708–713.
- [Goodman 1962] L. A. Goodman, “The variance of the product of  $K$  random variables”, *J. Amer. Stat. Assoc.* **57**:297 (1962), 54–60.
- [Grytz and Meschke 2009] R. Grytz and G. Meschke, “Constitutive modeling of crimped collagen fibrils in soft tissues”, *J. Mech. Behav. Biomed. Mater.* **2**:5 (2009), 522–533.
- [Gutsmann et al. 2004] T. Gutsmann, G. Fantner, J. Kindt, M. Venturoni, S. Danielsen, and P. Hansma, “Force spectroscopy of collagen fibers to investigate their mechanical properties and structural organization”, *Biophys. J.* **86**:5 (2004), 3186–3193.
- [Kastelic et al. 1978] J. Kastelic, A. Galeski, and E. Baer, “The multicomposite structure of tendon”, *Connect. Tissue Res.* **6**:1 (1978), 11–23.
- [Limbert 2011] G. Limbert, “A mesostructurally-based anisotropic continuum model for biological soft tissues—decoupled invariant formulation”, *J. Mech. Behav. Biomed. Mater.* **4**:8 (2011), 1637–1657.

- [Petruska and Hodge 1964] J. Petruska and A. Hodge, “A subunit model for the tropocollagen macromolecule”, *Proc. Nat. Acad. Sci. USA* **51**:5 (1964), 871–876.
- [Pins et al. 1997] G. Pins, E. Huang, D. Christiansen, and F. Silver, “Effects of static axial strain on the tensile properties and failure mechanisms of self-assembled collagen fibers”, *J. Appl. Polym. Sci.* **63**:11 (1997), 1429–1440.
- [Ross 2004] S. M. Ross, *Introduction to probability and statistics for engineers and scientists*, 3rd ed., Academic Press, Burlington, MA, 2004.
- [Thompson and Czernuszka 1995] J. I. Thompson and J. T. Czernuszka, “The effect of two types of cross-linking on some mechanical properties of collagen”, *Biomed. Mater. Eng.* **5**:1 (1995), 37–48.
- [Trombetta and Bradshaw 2010] J. M. Trombetta and A. D. Bradshaw, “SPARC/Osteonectin functions to maintain homeostasis of the collagenous extracellular matrix in the periodontal ligament”, *J. Histochem. Cytochem.* **58**:10 (2010), 871–879.
- [Wang et al. 1997] J. L. Wang, M. Parnianpour, A. Shirazi-Adl, and A. E. Engin, “Failure criterion of collagen fiber: Viscoelastic behavior simulated by using load control data”, *Theor. Appl. Fract. Mech.* **27**:1 (1997), 1–12.
- [Yamamoto et al. 1999] E. Yamamoto, K. Hayashi, and N. Yamamoto, “Mechanical properties of collagen fascicles from the rabbit patellar tendon”, *J. Biomech. Eng. (ASME)* **121**:1 (1999), 124–131.

Received 19 Feb 2014. Revised 16 Jun 2014. Accepted 14 Jul 2014.

FRANCESCO GENNA: francesco.genna@unibs.it

Department of Civil Engineering, University of Brescia, Via Branze 43, I-25123 Brescia, Italy

# JOURNAL OF MECHANICS OF MATERIALS AND STRUCTURES

[msp.org/jomms](http://msp.org/jomms)

Founded by Charles R. Steele and Marie-Louise Steele

## EDITORIAL BOARD

ADAIR R. AGUIAR	University of São Paulo at São Carlos, Brazil
KATIA BERTOLDI	Harvard University, USA
DAVIDE BIGONI	University of Trento, Italy
IWONA JASIUK	University of Illinois at Urbana-Champaign, USA
THOMAS J. PENCE	Michigan State University, USA
YASUhide SHINDO	Tohoku University, Japan
DAVID STEIGMANN	University of California at Berkeley

## ADVISORY BOARD

J. P. CARTER	University of Sydney, Australia
D. H. HODGES	Georgia Institute of Technology, USA
J. HUTCHINSON	Harvard University, USA
D. PAMPLONA	Universidade Católica do Rio de Janeiro, Brazil
M. B. RUBIN	Technion, Haifa, Israel

**PRODUCTION** [production@msp.org](mailto:production@msp.org)

SILVIO LEVY Scientific Editor

Cover photo: Wikimedia Commons

---

See [msp.org/jomms](http://msp.org/jomms) for submission guidelines.

---

JoMMS (ISSN 1559-3959) at Mathematical Sciences Publishers, 798 Evans Hall #6840, c/o University of California, Berkeley, CA 94720-3840, is published in 10 issues a year. The subscription price for 2014 is US \$555/year for the electronic version, and \$710/year (+\$60, if shipping outside the US) for print and electronic. Subscriptions, requests for back issues, and changes of address should be sent to MSP.

---

JoMMS peer-review and production is managed by EditFLOW<sup>®</sup> from Mathematical Sciences Publishers.

PUBLISHED BY

 **mathematical sciences publishers**  
nonprofit scientific publishing

<http://msp.org/>

© 2014 Mathematical Sciences Publishers

# Journal of Mechanics of Materials and Structures

Volume 9, No. 5

September 2014

---

**Buckling of two-phase inhomogeneous columns at arbitrary phase contrasts and volume fractions**

**MOHAMMED G. ALDADAH,  
SHIVAKUMAR I. RANGANATHAN and FARID H. ABED 465**

**A nonlinear stress-stretch relationship for a single collagen fibre in tension**

**FRANCESCO GENNA 475**

**Force–displacement relationship in the extraction of a porcine tooth from its socket: experiments and numerical simulations**

**FRANCESCO GENNA and CORRADO PAGANELLI 497**

**Nonuniform shear strains in torsional Kolsky bar tests on soft specimens**

**ADAM SOKOLOW and MIKE SCHEIDLER 515**

**Transient elastic-viscoplastic dynamics of thin sheets**

**ALI A. ATAI and DAVID J. STEIGMANN 557**



1559-3959(2014)9:5;1-5